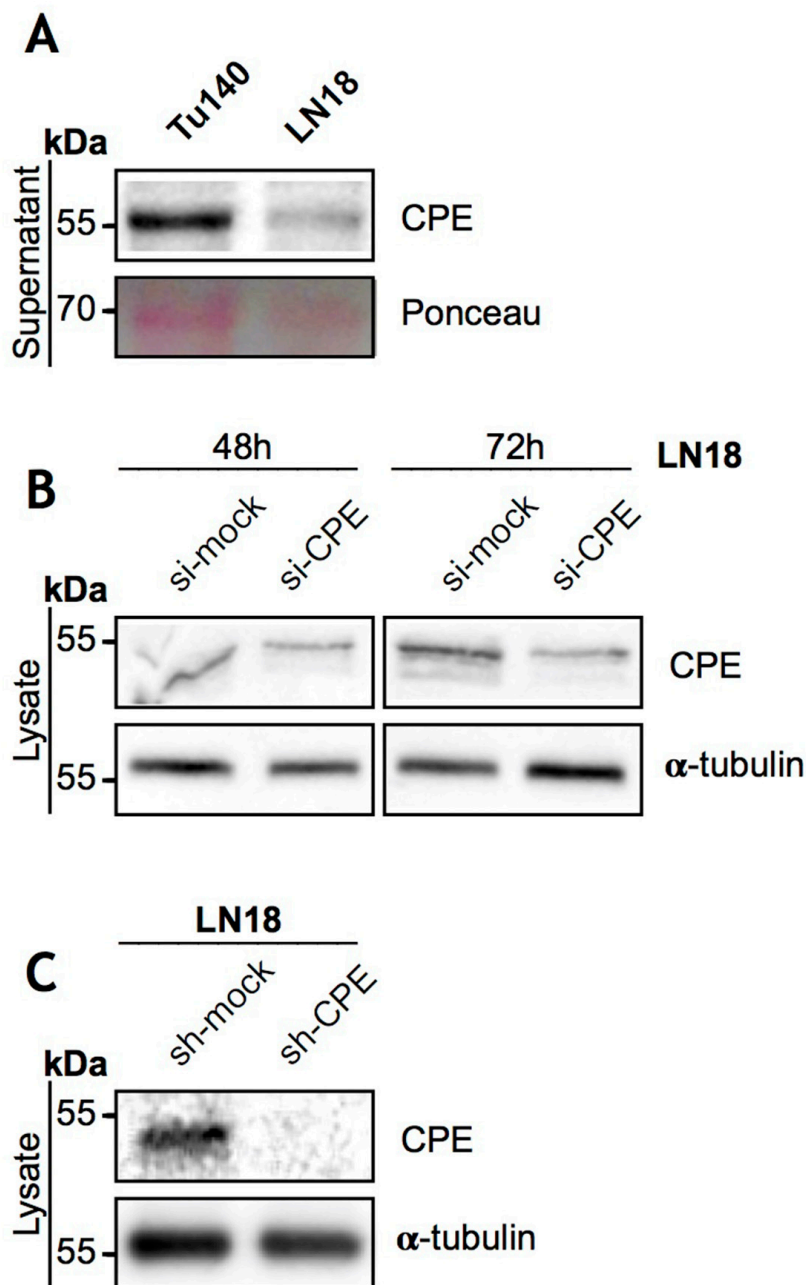
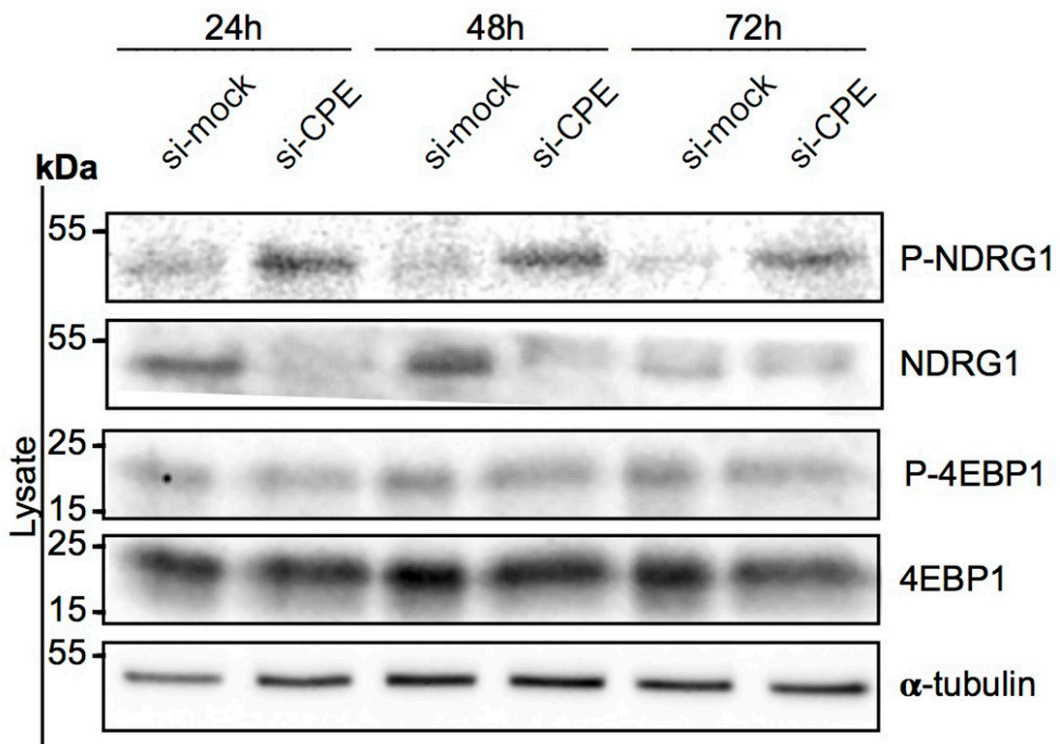


Effects of soluble CPE on glioma cell migration are associated with mTOR activation and enhanced glucose flux

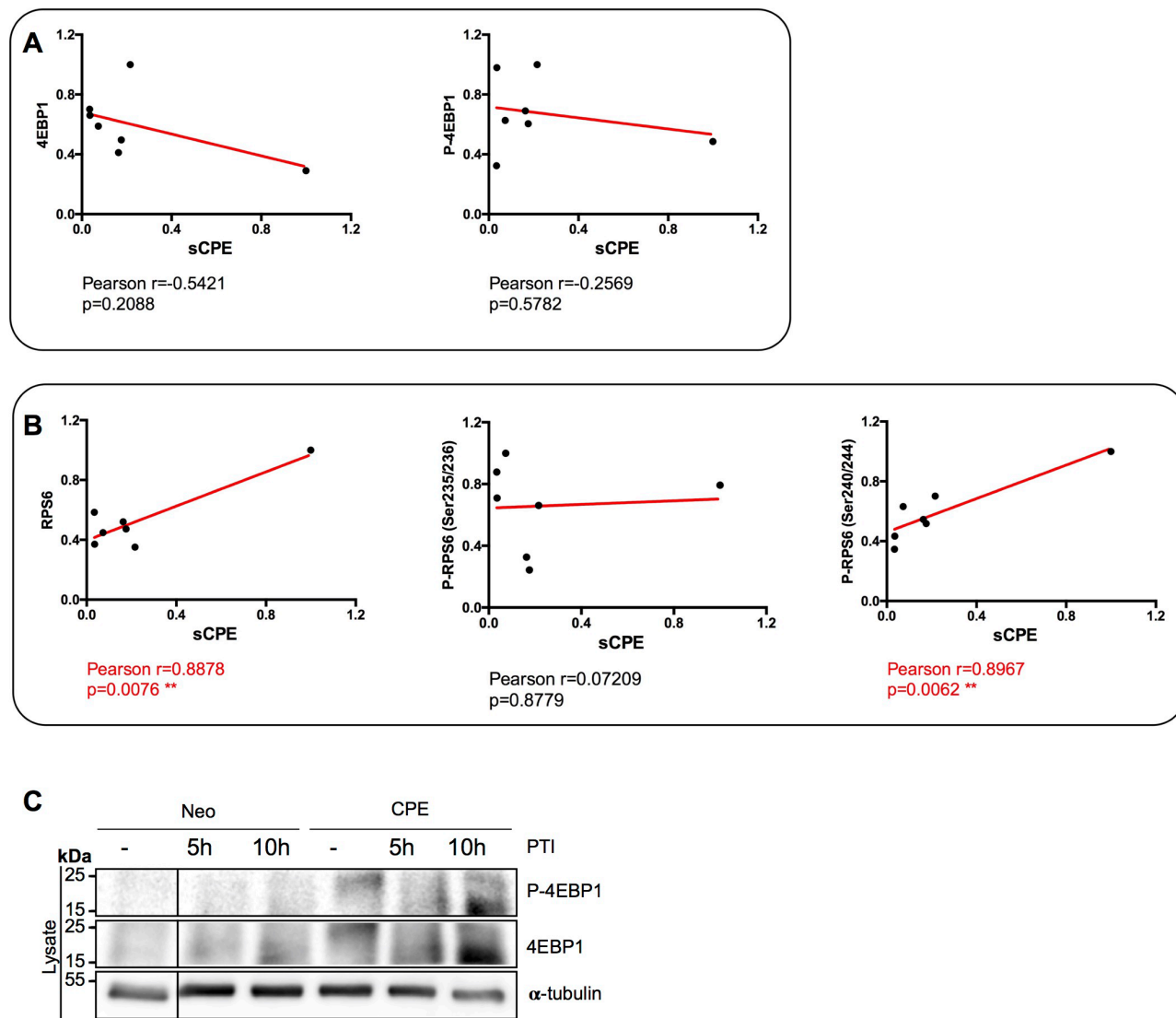
SUPPLEMENTARY MATERIALS



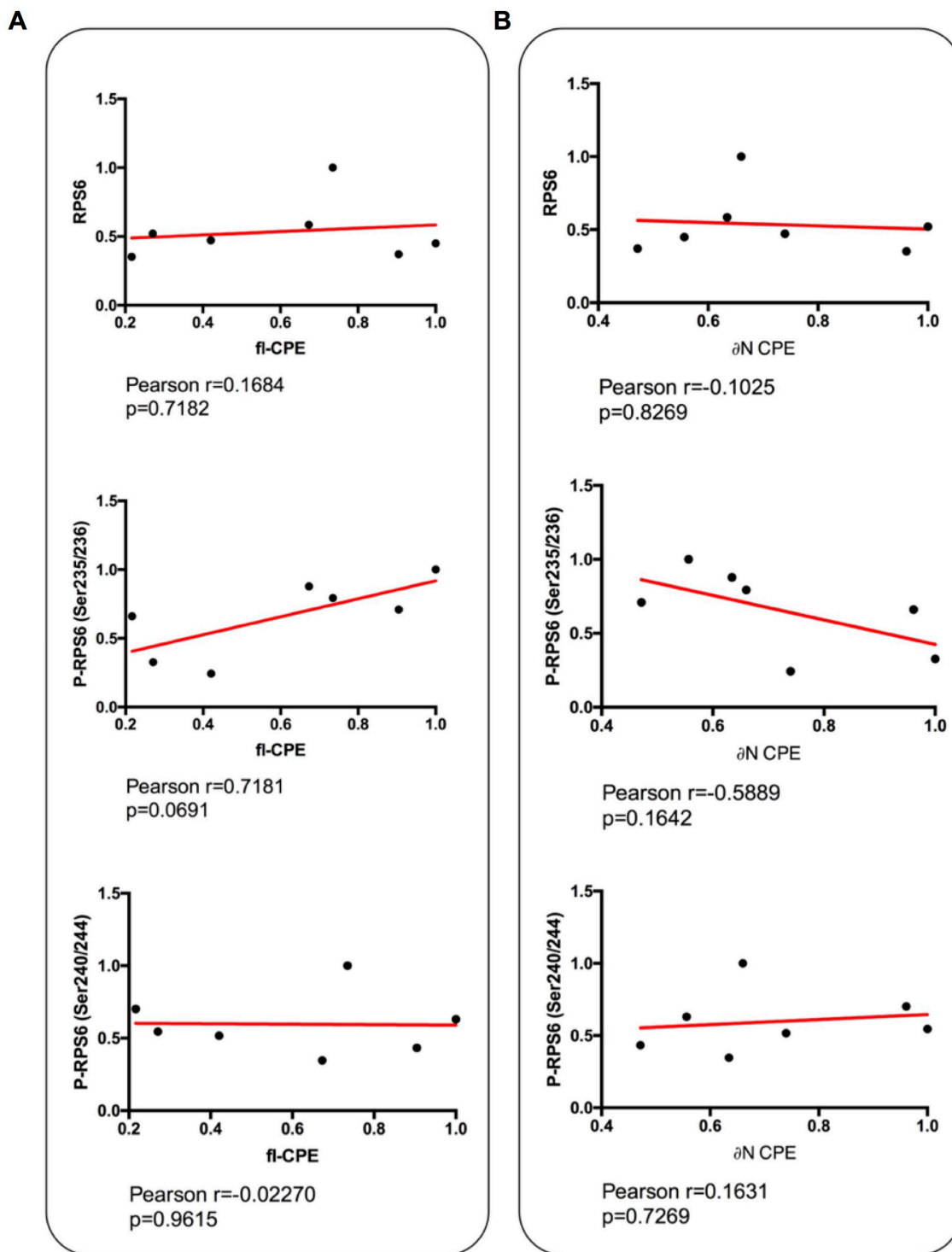
Supplementary Figure 1: Tu140 and LN18 cells secrete CPE. (A) Immunoblot detection of sCPE obtained from the supernatants of the parental Tu140 and LN18 GBM cells. Ponceau staining was used as a loading control. The cells were serum-starved for 24h in serum-reduced medium prior to supernatant collection. A representative immunoblot is shown. (B, C) Representative immunoblots for detection of CPE in the (B) transient or (C) stable CPE knockdown in the LN18 cells. Control si- or shRNA (si-mock/sh-mock) were used as negative controls. α -tubulin was used as a loading control.



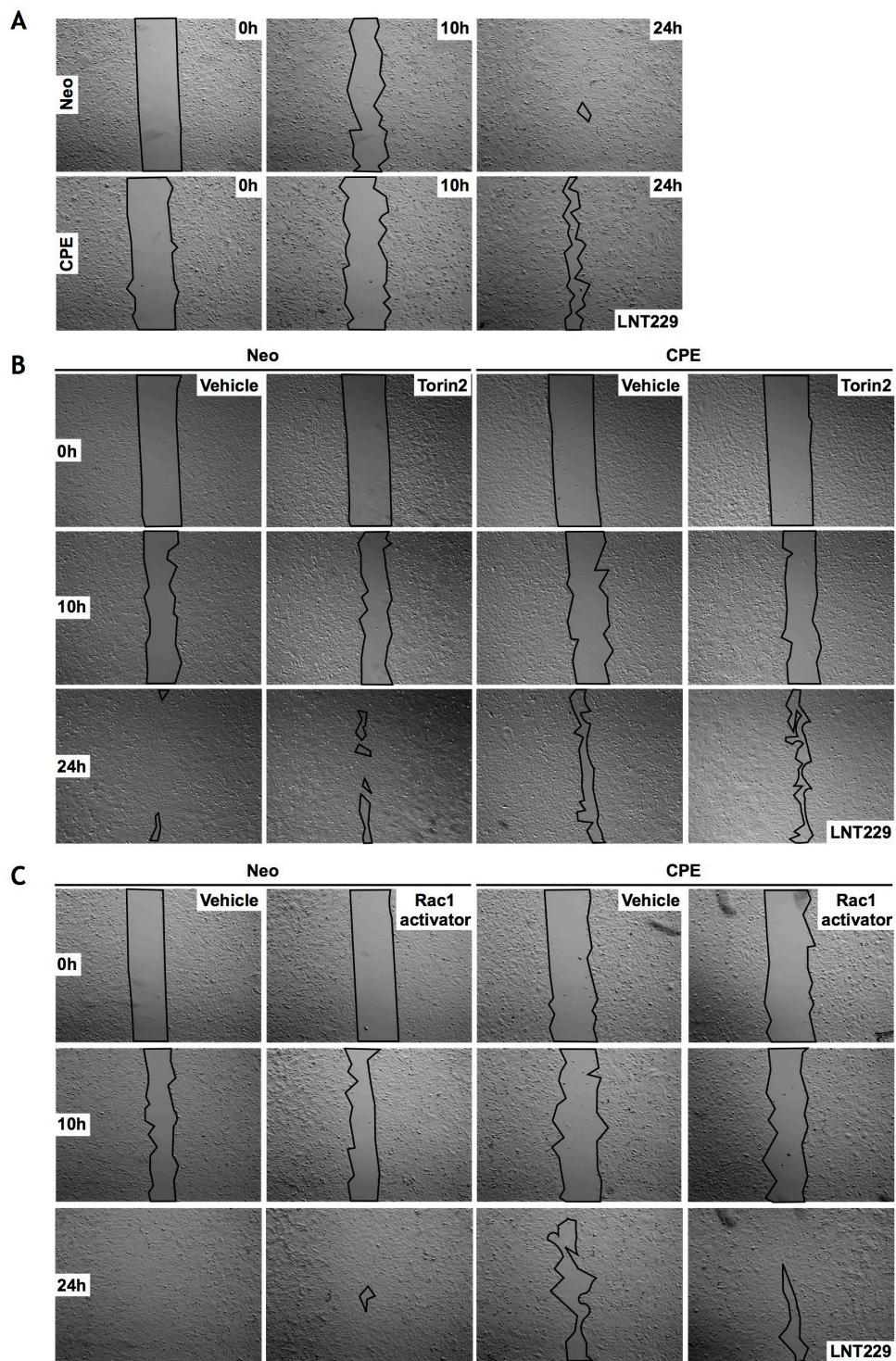
Supplementary Figure 2: Signaling profiling of Tu140 cells. Representative immunoblots for detection of phosphorylated and total amounts of NDRG1 and 4EBP1 in the CPE-knockdown primary GBM Tu140 cells. Control siRNA (si-mock) was used as negative control. α -tubulin was used as a loading control.



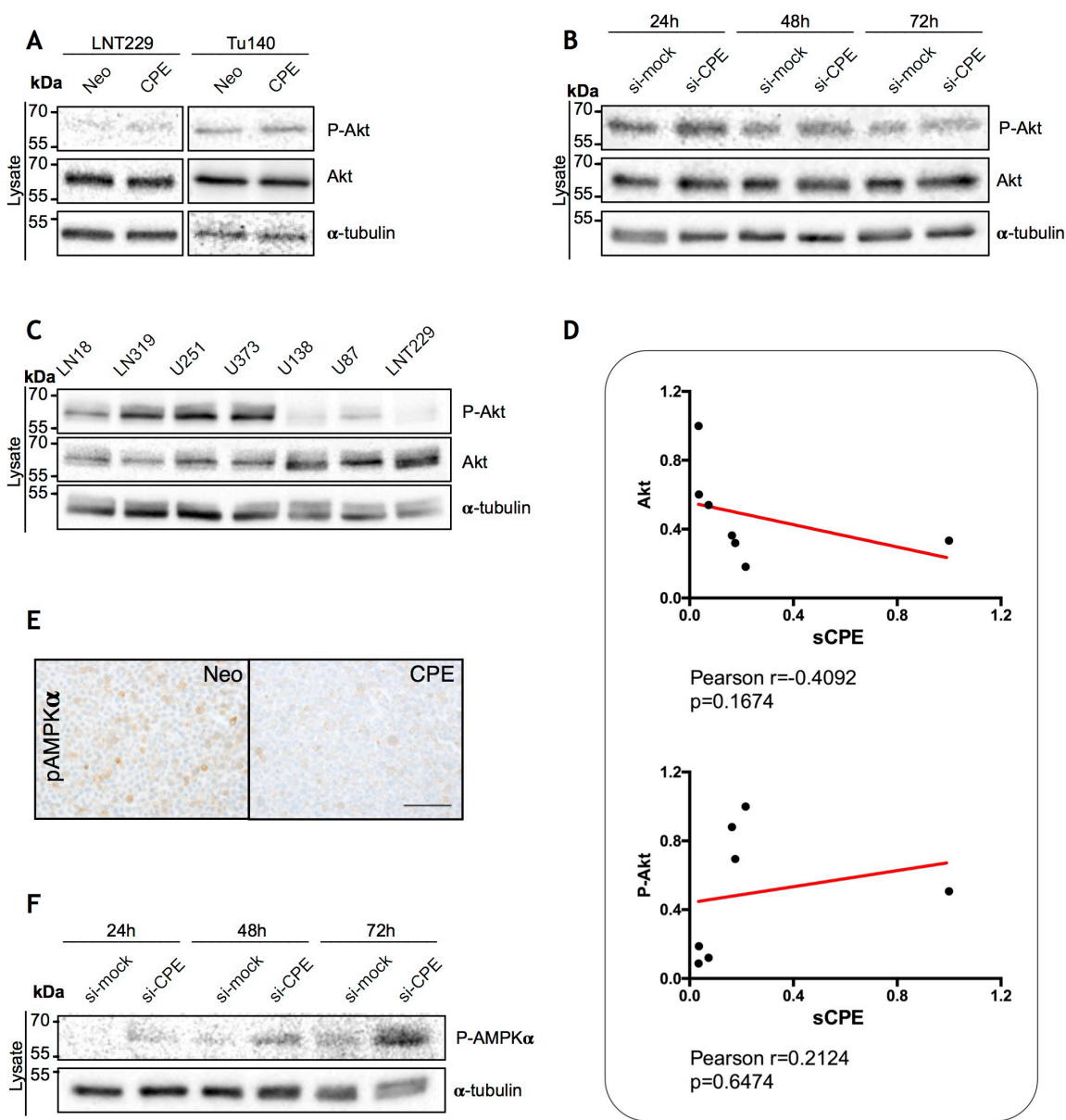
Supplementary Figure 3: CPE secretion is necessary to activate RPS6. (A, B) Correlation analysis of densitometric measurements of immunoblotting results in 7 GBM cell lines between sCPE and total as well as phosphorylated forms of (A) 4EBP1 and (B) RPS6. Pearson coefficients and exact p-values are shown (** $p<0.01$). (C) Detection of 4EBP1 and its phosphorylation in the lysates of the Neo or sCPE-overexpressing LNT229 cell line. The cells were serum-starved for 5h in serum-reduced medium (without treatment) or for 5h and 10h in serum-reduced medium with 1x protein transport inhibitor (PTI) cocktail prior to lysis. A representative immunoblot is shown. α -tubulin was used as a loading control.



Supplementary Figure 4: flCPE and Δ N-CPE do not correlate with RPS6 in GBM cells. (A, B) Correlation analysis of densitometric measurements of immunoblotting results in 7 GBM cell lines between (A) flCPE and RPS6 and its phosphorylation form or (B) between Δ N-CPE and RPS6.



Supplementary Figure 5: Wound-healing assay in LNT229 sCPE-overexpressing cells. (A-C) Representative experiments, showing closure of the cell-free gap by sCPE-overexpressing or corresponding control (Neo) LNT229 cells over 24h under (A) standard conditions, (B) treatment with Torin2 and (C) treatment with Rac1 activator.



Supplementary Figure 6: Potential intracellular mediators of sCPE effects on glioma cell migration. (A) Representative immunoblots for detection of phosphorylated and total amounts of Akt in the sCPE-overexpressing vs. Neo LNT229 and Tu140 cell lysates. α -tubulin was used as a loading control. The cells were serum-starved for 24h in serum-reduced medium prior to lysis. (B) Representative immunoblots for detection of phosphorylated and total amounts of Akt in the CPE-knockdown primary GBM Tu140 cells. Control siRNA (si-mock) was used as negative control. α -tubulin was used as a loading control. (C) Signaling profiling of 7 GBM cell lines. Immunoblot detection of Akt levels and its phosphorylation in the lysates derived from 7 GBM cell lines. α -tubulin were used as loading control. The cells were serum-starved for 24h in serum-reduced medium prior to lysis. Representative immunoblots are shown. (D) Correlation analysis of densitometric measurements of immunoblotting results in 7 GBM cell lines between sCPE and total as well as phosphorylated forms of Akt. Pearson coefficients and exact p-values are shown. (E) Immunohistochemical staining of pAMPK α in the Neo or sCPE-overexpressing LNT229 cells (20x magnification, scale bar 100 μ m). (F) A representative immunoblot for detection of phosphorylated AMPK α in the CPE-knockdown primary GBM Tu140 cells. Control siRNA (si-mock) was used as negative control. α -tubulin was used as a loading control.

Supplementary Table 1: MS-based phosphoproteomic analysis in LNT229 glioma cells upon sCPE overexpression

See Supplementary File 1